Psychological Medicine (2017), **47**, 639–654. © Cambridge University Press 2016
doi:10.1017/S0033291716002695

ORIGINAL ARTICLE

Shared atypical brain anatomy and intrinsic functional architecture in male youth with autism spectrum disorder and their unaffected brothers

H.-Y. Lin[1], W.-Y. I. Tseng[2,3], M.-C. Lai[1,4,5], Y.-T. Chang[6] and S. S.-F. Gau[1,3]*

[1] *Department of Psychiatry, National Taiwan University Hospital and College of Medicine, Taipei, Taiwan*
[2] *Institute of Medical Devices and Imaging System, National Taiwan University College of Medicine, Taipei, Taiwan*
[3] *Graduate Institute of Brain and Mind Sciences, National Taiwan University College of Medicine, Taipei, Taiwan*
[4] *Department of Psychiatry, Child and Youth Mental Health Collaborative at the Centre for Addiction and Mental Health and The Hospital for Sick Children, University of Toronto, Toronto, Ontario, Canada*
[5] *Department of Psychiatry, Autism Research Centre, University of Cambridge, Cambridge, UK*
[6] *McGovern Institute for Brain Research, Massachusetts Institute of Technology, Cambridge, MA, USA*

Background. Autism spectrum disorder (ASD) is a highly heritable neurodevelopmental disorder, yet the search for definite genetic etiologies remains elusive. Delineating ASD endophenotypes can boost the statistical power to identify the genetic etiologies and pathophysiology of ASD. We aimed to test for endophenotypes of neuroanatomy and associated intrinsic functional connectivity (iFC) via contrasting male youth with ASD, their unaffected brothers and typically developing (TD) males.

Method. The 94 participants (aged 9–19 years) – 20 male youth with ASD, 20 unaffected brothers and 54 TD males – received clinical assessments, and undertook structural and resting-state functional magnetic resonance imaging scans. Voxel-based morphometry was performed to obtain regional gray and white matter volumes. A seed-based approach, with seeds defined by the regions demonstrating atypical neuroanatomy shared by youth with ASD and unaffected brothers, was implemented to derive iFC. General linear models were used to compare brain structures and iFC among the three groups. Assessment of familiality was investigated by permutation tests for variance of the within-family pair difference.

Results. We found that atypical gray matter volume in the mid-cingulate cortex was shared between male youth with ASD and their unaffected brothers as compared with TD males. Moreover, reduced iFC between the mid-cingulate cortex and the right inferior frontal gyrus, and increased iFC between the mid-cingulate cortex and bilateral middle occipital gyrus were the shared features of male ASD youth and unaffected brothers.

Conclusions. Atypical neuroanatomy and iFC surrounding the mid-cingulate cortex may be a potential endophenotypic marker for ASD in males.

Received 11 December 2015; Revised 16 September 2016; Accepted 16 September 2016; First published online 9 November 2016

Key words: Autism spectrum disorder, endophenotypes, intrinsic functional connectivity, resting-state functional magnetic resonance imaging, unaffected siblings.

Introduction

Autism spectrum disorder (ASD) is a childhood-onset neurodevelopmental disorder, with strong heritability (Colvert *et al.* 2015; Kim & Leventhal, 2015) and familial aggregation (Sucksmith *et al.* 2011; Sandin *et al.* 2014). Attempts to find genetic variants that link to ASD susceptibility yield inconsistent results, owing substantially to phenotypic heterogeneity (Geschwind & State, 2015). To aid the identification of more homogeneous subgroups within the autistic spectrum and to increase statistical power to detect susceptible genes, researchers turn to endophenotypes, the intermediate components connecting genotype and behavioral phenotypes. Endophenotypes are quantifiable traits associated with a disorder. They are heritable and present in biological relatives (e.g. unaffected siblings) at a higher rate than in the general population (Gottesman & Gould, 2003; Glahn *et al.* 2014). Features shared by individuals with ASD and their siblings at the brain level are potential endophenotypes for identifying mechanisms leading to ASD.

Neuroimaging data provide evidence for atypical brain growth trajectories in ASD involving the

* Address for correspondence: S. S.-F. Gau, Department of Psychiatry, National Taiwan University Hospital and College of Medicine, No. 7, Chung-Shan South Road, Taipei, 10002, Taiwan.
(Email: gaushufe@ntu.edu.tw)

frontotemporal, frontoparietal and frontostriatal circuitries, anterior and posterior cingulate cortices, the amygdala–hippocampal complex and cerebellum (Amaral *et al.* 2008; Ecker *et al.* 2015). These regions are heavily implicated in specific clinical symptoms (Courchesne *et al.* 2007; Amaral *et al.* 2008; D'Mello *et al.* 2015). Structural magnetic resonance imaging (MRI) studies also suggest that the atypical neuroanatomy of ASD is sex- (Lai *et al.* 2013; Schaer *et al.* 2015; Supekar & Menon, 2015) and age-dependent (Nickl-Jockschat *et al.* 2012; Lin *et al.* 2015). Atypical neuroanatomy of ASD lies beyond widespread local changes but also involves inter-regional brain connectivity (Schipul *et al.* 2011). At the functional level, these were once posited as short-range over-connectivity and long-range under-connectivity (Belmonte *et al.* 2004; Wass, 2011). Emerging literature on intrinsic functional connectivity (iFC) suggests unique patterns of both under- and over-connectivity in ASD with regional specificity (Di Martino *et al.* 2014; Fishman *et al.* 2014). Recent attempts to resolve conflicting findings have delineated methodological (Müller *et al.* 2011), conceptual (Vissers *et al.* 2012) and developmental (Uddin *et al.* 2013) issues. A multimodal structural and functional imaging approach might be able to detect informative super-regional neural characteristics jointly in ASD (Mueller *et al.* 2013).

First-degree relatives of individuals with ASD may display mild autistic traits, including communication and social difficulties, alongside rigid personality, interests and behavior (Sucksmith *et al.* 2011). Biological full siblings of individuals with ASD are about 10 times more likely to develop ASD than the general population (Sucksmith *et al.* 2011; Sandin *et al.* 2014). These findings indicate that some unaffected siblings of individuals with ASD inherit the associated genetic predisposition for ASD, and they may have the broader autism phenotype. As genetic factors are responsible for a significant amount of variation in neuroanatomy (Giedd *et al.* 2010; Blokland *et al.* 2012; Hibar *et al.* 2015) and iFC (Glahn *et al.* 2010; Fornito *et al.* 2011) in neurotypical individuals, shared alterations in brain morphology and associated iFC between individuals with ASD and their unaffected siblings is likely to be an informative endophenotype.

Some studies have investigated brain structural differences in relatives of people with ASD. Relative to controls, reduced amygdala volume reduction and larger left hippocampus volumes were reported in unaffected siblings (Dalton *et al.* 2007) and unaffected parents (Rojas *et al.* 2004) of individuals with autism, respectively. However, Peterson *et al.* (2006), using voxel-based morphometry (VBM), failed to replicate these, while they reported increased gray matter (GM) volume of the inferior and middle frontal gyrus and cerebellum in parents of children with autism. Contrary to the findings mentioned above, Palmen *et al.* (2005) did not detect any significant differences in any brain regions in parents of ASD probands. Earlier literature also reports no differences in total brain (Rojas *et al.* 2004; Peterson *et al.* 2006) and corpus callosum volume (Branchini *et al.* 2009) between unaffected relatives and controls. Using the same participant cohort, Segovia *et al.* (2014) applied a multivariate approach and reported that cerebellum volume could be a candidate neuroendophenotype; Moseley *et al.* (2015) suggested that whole-brain functional hypoconnectivity in task and rest conditions may be an endophenotype of ASD in adolescents; Spencer *et al.* (2012) reported local endophenotypic effects in visual processing and default mode networks. Despite respective evidence of brain structural and functional differences in autism relatives, to the best of our knowledge, analysis of shared alterations in brain structures and associated shared iFC between autistic probands and their unaffected siblings has not been implemented. As atypical neuroanatomical findings may result in atypical functions and functional connectivity patterns, this dearth of integrative evidence limits functional interpretations of brain morphological studies, and eludes direct explorations of neuroimaging endophenotypes of ASD.

This study thus aimed to examine the hypothesis that individuals with ASD and their unaffected siblings share alterations in GM and white matter (WM) volume, and the associated iFC is also shared by individuals with ASD and their unaffected siblings. Given that brain structural differences in autism are modulated by sex (Lai *et al.* 2013; Schaer *et al.* 2015; Supekar and Menon, 2015), we focused only on male participants to build upon limited literature about neuroimaging endophenotypes of ASD. We also tested whether these shared differences were associated with behavioral characteristics of ASD.

Method

Procedure

The Research Ethics Committee at the National Taiwan University Hospital (NTUH) approved this study before implementation (approval number: 201201006RIB; ClinicalTrials.gov number, NCT01582256). The procedures and purpose of the study were explained face to face to the participants and their parents, who then provided written informed consent. All participants underwent the same clinical and MRI assessments; the ASD group additionally received the

Chinese version of the Autism Diagnostic Interview-Revised (ADI-R) assessment (Gau *et al.* 2010).

Participants and measures

We recruited 94 Taiwanese male participants [aged 8–19 years, full-scale intelligence quotient (FSIQ) 75–148], including males with ASD and their unaffected full biological brothers in 20 simplex families, consecutively from the child psychiatry out-patient clinic of NTUH. We also recruited 54 typically developing (TD) males matched for age from similar geographical districts, without a family history of ASD. Participants with ASD were clinically diagnosed according to Diagnostic and Statistical Manual of Mental Disorders, 4th Edition, Text Revision (DSM-IV-TR) and International Statistical Classification of Diseases and Related Health Problems, 10th Revision (ICD-10) criteria and further confirmed by the ADI-R (Rutter *et al.* 2003; Gau *et al.* 2010). All unaffected brothers and TD males were also clinically assessed to confirm that they did not have a diagnosis of ASD. All participants and their parents received an interview using the Chinese version of the Kiddie epidemiologic version of the Schedule for Affective Disorders and Schizophrenia (Gau *et al.* 2005) to exclude any current or lifetime DSM-IV-TR psychiatric disorder. Exclusion criteria for all groups included past or current neurological or severe medical illness (e.g. tic, epilepsy), substance use disorders, schizophrenia, attention-deficit/hyperactivity disorder, lifetime diagnoses of mood disorders, current anxiety disorders, current use of psychotropic medication, FSIQ <70.

Intellectual function was assessed by the Wechsler Intelligence Scale for Children–3rd Edition (Wechsler, 1991) in participants aged 16 years or younger, or by the Wechsler Adult Intelligence Scale–3rd Edition (Wechsler, 1997). Handedness was assessed by the Edinburgh Inventory (Oldfield, 1971). Autistic traits were assessed by the Chinese version of the Social Responsiveness Scale (SRS) (Gau *et al.* 2013), the Autism Spectrum Quotient (AQ)-Chinese (Lau *et al.* 2013) and the Social Communication Questionnaire (SCQ) (Gau *et al.* 2011). The Chinese SRS (Gau *et al.* 2013), AQ (Lau *et al.* 2013) and SCQ (Gau *et al.* 2011) have well-accepted psychometric properties for measuring autistic features in the Taiwanese population (Hsiao *et al.* 2013; Kuo *et al.* 2014; Lau *et al.* 2014). Confirmatory factor analysis revealed a four-factor structure of the Chinese SRS, namely 'social communication', 'autism mannerism', 'social awareness' and 'social emotion' (Gau *et al.* 2013). The AQ-Chinese, simplified from the original version of the AQ (Baron-Cohen *et al.* 2001), comprises 35 items with five dimensional factors, including 'socialness', 'mindreading', 'patterns', 'attention to detail' and 'attention switching' (Lau *et al.* 2013).

MRI acquisition and preprocessing

High-resolution T1-weighted images and echo planar imaging (EPI) were acquired on a 3 T MRI scanner (Siemens Magnetom Tim Trio) using a 32-channel phased-arrayed head coil. Three-dimensional magnetization prepared rapid acquisition gradient echo sequence parameters were: repetition time (TR) = 2000 ms; echo time (TE) = 2.98 ms; inversion time (TI) = 900 ms; flip angle = 9°; field of view (FOV) = 256 × 256 mm^2; matrix size = 256 × 256 × 192; voxel size = 1 mm^3 isotropic. To complete a 6-min resting-state functional MRI (rs-fMRI) scan, all participants were verbally instructed to remain still with their eyes closed (Van Dijk *et al.* 2010). Wakefulness was monitored and ensured at the end of the scan by checking the participants' prompt responses to technicians' questions. All participants denied falling into sleep during scanning. The resting EPI parameters were: 180 volumes; TR = 2000 ms; TE = 24 ms; flip angle = 90°; FOV = 256 × 256 mm^2; matrix size = 64 × 64; 34 axial slices acquired in an interleaved descending order; slice thickness = 3 mm; voxel size = 4 × 4 × 3 mm^3; imaging plane being parallel to the anterior commissure–posterior commissure (AC–PC) image plane.

Structural imaging preprocessing and VBM

Before preprocessing, we visually inspected structural image data to confirm no anatomical lesions, nor imaging artefacts, and ensure data quality without excessive in-scanner head motion in all participants. Individual T1-weighted images were segmented by the New Segment toolbox in SPM8 (Wellcome Trust Centre for Neuroimaging, UK) to produce native space GM, WM and cerebral spinal fluid (CSF) images. During segmentation, for all individuals below the age of 18 years, age- and sex-matched study-specific tissue probability maps generated from the Template-O-Matic toolbox (using the 'matched-pair' approach) were used (Wilke *et al.* 2008); for individuals above 18 years old, the default tissue probability map in New Segment was used. The native-space GM and WM images of all participants were then registered to a study-specific template using a high-dimensional non-linear diffeomorphic registration algorithm (DARTEL) (Ashburner, 2007), with modulation (preserve volume). The modulated GM and WM maps were smoothed with a 4 mm full width at half maximum (FWHM) Gaussian kernel. Individual total GM, WM and CSF volumes were estimated by summing up the partial volume estimates throughout each class of segmented image in the native space.

Total brain volumes were estimated by summing up total GM and WM volumes.

rs-fMRI imaging preprocessing

Standard echo-planar imaging (EPI) preprocessing was performed using the DPARSF toolbox (Yan & Zang, 2010) based on SPM8. The first five EPI volumes were discarded to allow for signal equilibration. Functional images were slice timing corrected, and each volume was realigned to the first image volume using a least-squares minimization and a six-parameter (rigid-body) spatial transformation. Participants were excluded if their translation and rotation realignment estimates were >1.5 mm and >1.5°. Realigned EPI image were then co-registered to structural scans, normalized to a Montreal Neurological Institute (MNI) template in isotropic 3 mm voxels via the GM segment, and smoothed with an 8 mm FWHM Gaussian kernel.

Prior to temporal filtering, we calculated the frame-wise displacement (FD) of in-scanner head motion based on the measures derived from Jenkinson and colleagues (Jenkinson *et al.* 2002; Yan *et al.* 2013*a*), to further ensure all EPI data did not exhibit maximum FD >1.5 mm. Participants with mean FD greater than 2 standard deviations above the mean motion of all participants (threshold: 0.257 mm) were further excluded for iFC analyses (Yan *et al.* 2013*b*), leaving 18 participants with ASD, 20 brothers and 48 TD males after two-stage exclusion based on the in-scanner motion criterion (online Supplementary Table S1). The smoothed fMRI data were denoised by implementing the Independent Component Analysis-based strategy for Automatic Removal of Motion Artifacts (ICA-AROMA) (Pruim *et al.* 2015*a*, *b*). After motion denoising, the EPI data were further denoised using the CONN toolbox v.15c (Whitfield-Gabrieli & Nieto-Castanon, 2012) to remove other resources of non-neural noises through a component-based (anatomical CompCor) approach (Behzadi *et al.* 2007). The first three principal components of the signals from the WM and CSF regions of interest (ROI) (anatomical masks derived from the prior segmentation steps), and linear detrending were included as regressors in the first-level denoising regression model. All of the regressors were filtered before performing the denoising regression (Hallquist *et al.* 2013). Temporally band-pass filtering (0.01–0.08 Hz) was performed simultaneously with regression ('Simult').

Statistical analyses of VBM

For all imaging analyses, an unbiased whole-brain approach was used to explore group differences. Group-level VBM was performed with SPM8 using the general linear model, with FSIQ, age (Ecker *et al.* 2015; Lin *et al.* 2015) and tissue-specific volume (i.e. total GM volume for GM analysis) included as covariates. Age × group interactions were similarly examined, but were not significant and thus excluded from the model.

Conjunction analysis testing using SPM8 of the minimum *t*-statistic over two orthogonal contrasts for regional neuroanatomical differences at cluster level was used. Only clusters surviving at family-wise error (FWE) $p < 0.05$ using random field theory, corrected for non-stationarity (Hayasaka & Nichols, 2003) at cluster level with a cluster-forming threshold of 0.005, were reported. Conjunction analysis testing for global differences (Friston *et al.* 1999, 2005) allows testing the null hypothesis of no differences between ASD individuals *v.* TD males and unaffected brothers *v.* TD males. To identify increased brain volume in the ASD group and their unaffected brothers compared with the TD group, the conjoined contrasts were (ASD > TD males: 1 0 −1; Brother > TD males: 0 1 −1). Conjunction analyses to detect decreased brain volume in the ASD group and their unaffected brothers compared with TD males were carried out with the conjoined contrasts as (ASD < TD males: −1 0 1; Brother < TD males: 0 −1 1) [a similar approach has been implemented in Belton *et al.* (2003) and Pironti *et al.* (2014)].

iFC and statistical analyses

To investigate the functional implications of the shared brain structural differences among ASD and brothers, we employed a seed-based approach to investigate iFC based on the GM cluster surviving conjunction analyses of VBM, the mid-cingulate cortex (MCC). The peak coordinates of the identified GM cluster were extracted and defined as *a priori* seeds with a 5-mm radius. Whole-brain functional connectivity was calculated by correlating the seed time-series with the time course of all other voxels using the RESting-state fMRI data analysis Toolkit (REST) toolbox (Song *et al.* 2011). The resulting Pearson's correlation coefficients were Fisher-*z* transformed to conform to normality assumptions for second-level analyses.

Group-level analyses of iFC were identical with the VBM approach, using general linear models with FSIQ, age and mean FD (Yan *et al.* 2013*a*) as nuisance covariates. Conjunction analyses based on a global null hypothesis (Friston *et al.* 1999, 2005) were implemented to identify shared atypical iFC by individuals with ASD and their brothers. The threshold of cluster-level inferences for conjunction analyses was also the same with those in VBM, i.e. a cluster-forming threshold of 0.005, and a cluster-level FEW-corrected

$p < 0.05$ for the minimum *t*-statistic over two orthogonal contrasts. Owing to the finite spatial coverage of the EPI scan, we excluded the cerebellum in the analysis by subtracting the cerebellum ROIs in the Automated Anatomical Labeling template (Tzourio-Mazoyer *et al.* 2002) from the GM mask.

To characterize differences between the three groups, clusters surviving the conjunction analyses were extracted and imported into SPSS to perform analysis of variance with 'group' (ASD, Brother, TD) as a fixed factor and cluster regional volume estimates or iFC as the dependent variable. All brain coordinates were given in the MNI convention. The xjView8 toolbox (http://www.alivelearn.net/xjview8/) was used to localize the significant GM clusters and the related Brodmann area (BA). WM structures were labeled by overlaying the significant clusters with standard space defined from JHU diffusion-tensor-imaging-based WM atlases (Wakana *et al.* 2007; Hua *et al.* 2008). The results were visualized using BrainNet Viewer (Xia *et al.* 2013) and MRIcroN (Rorden *et al.* 2007).

As the analysis of covariance may not adjust for a pre-existing between-group difference in IQ, which is a correlated covariate (Suckling, 2011) with the independent variable 'group', we employed subsidiary analyses using models without covarying FSIQ for both structural and iFC comparisons (online Supplementary Fig. S1). To further allow comparisons with the earlier literature in the field, the results of the non-conjoined analysis (i.e. ASD *v.* TD and Brother *v.* TD, respectively) are also presented in the online Supplementary Results.

Assessment of familiality

Based on a published method (Menzies *et al.* 2007; Ersche *et al.* 2012), we calculated the variance of the within-family-pair difference in brain measures: σ (ASD proband–Brother pair) $= \sum(u_j - \bar{u})^2/N$. u_j is the within-pair difference of the measures for the j^{th} pair of participants; $\bar{u}$ is the mean of the within-pair differences; N is the total number of the pairs ($n = 20$ for structural measures; $n = 18$ for iFC). Then the new pairs were randomly reassigned to make each participant paired with an unaffected brother to whom they were not personally related. The variance of the within-pair difference in the randomized sibling pair was calculated after each random re-pairing. This process was repeated 1 000 000 times to sample the permutation distribution of σ (ASD proband–Brother pair) under the null hypothesis that the observed variance of within-pair differences was not determined by the familiality of the observed pairs. On the alternative hypothesis that the observed variance would be small, this was compared with the 50 000th value of the permutation distribution for a one-tailed test of the null hypothesis with $p < 0.05$.

Correlations of GM and WM volumetric differences and altered iFC with autistic symptoms

Besides regional volume estimates of shared GM and WM differences, the iFC strength (*z*-transformed correlation) in each cluster with a significant conjoined difference was extracted from each participant. To investigate the association of volume estimates and altered iFC with autistic symptoms, respectively, bivariate Pearson's correlation was employed separately for each group. Autistic symptoms were encapsulated as the regression factor derived from a principal component analysis of the total scores of the Chinese SRS, Chinese SCQ and AQ-Chinese. The first principal component was extracted, which explained 97.01% of the variance. This was decided based on eigenvalues, cumulative variance and inspection of the scree plot. Factors were orthogonally rotated using Varimax rotation. Pearson's correlations and principal component analysis were implemented using IBM SPSS Statistics for Macintosh, version 22.0 (IBM Corp., USA).

Ethical standards

All procedures contributing to this work comply with the ethical standards of the relevant national and institutional committees on human experimentation and with the Helsinki Declaration of 1975, as revised in 2008.

Results

Demographic and clinical characteristics

The three groups did not differ in age or handedness. The ASD group differed from the Brother and TD groups in FSIQ and verbal IQ, alongside parent-reported autistic symptoms regarding total scores of the Chinese SRS, Chinese SCQ and AQ-Chinese (Table 1). In participants qualified for resting-state fMRI analysis, these patterns remained the same (online Supplementary Table S1). There were no significant differences in in-scanner motion composites in terms of mean FD, time point exhibiting FD > 0.5 mm, alongside root mean squared head position change, among the three groups (Table 1).

Neuroimaging analyses

Multivariate analysis of covariance assessing for GM, WM and total brain volume with group as a fixed factor and age and FSIQ as covariates showed no differences between the three groups (GM: $F_{2,89} = 1.06$,

Table 1. *Demographic characteristics of the participants*

	ASD youth ($n = 20$)	Unaffected brothers ($n = 20$)	TD males ($n = 54$)	Statistics	Comparisons
Age (range 8–19 years), years	13.3 (2.5)	14.4 (3.1)	12.8 (2.6)	$F = 2.42$; $p = 0.095$	
Handedness, right, *n* (%)	19 (95)	20 (100)	50 (92.6)	$\chi^2 = 1.60$; $p = 0.450$	
IQ					
Full-scale IQ	103.8 (17.8)	112.0 (10.4)	112.5 (11.6)	$F = 5.55$; $p = 0.006$	ASD < Brother, TD
Verbal IQ	103.6 (16.6)	113.2 (11.5)	111.7 (10.5)	$F = 6.83$; $p = 0.002$	ASD < Brother, TD
Performance IQ	103.7 (17.9)	108.9 (10.9)	111.7 (13.7)	$F = 2.45$; $p = 0.095$	–
Autism Diagnostic Interview-Revised[a]					
Social reciprocity	19.1 (6.5)	–	–	–	–
Communication, verbal	15.2 (5.1)	–	–	–	–
Stereotyped behavior	7.9 (2.2)	–	–	–	–
Social Responsiveness Scale, parent-report[b]					
Total	87.9 (39.8)	29.1 (17.7)	27.1 (12.24)	$F = 54.05$; $p < 0.001$	ASD > Brother, TD
Social Communication Questionnaire[c]					
Total	17.6 (8.4)	3.6 (3.6)	3.8 (2.8)	$F = 57.46$; $p < 0.001$	ASD > Brother, TD
Autism Spectrum Quotient[d]					
Total	139.8 (18.9)	102.0 (18.6)	108.0 (13.0)	$F = 29.96$; $p < 0.001$	ASD > Brother, TD
Motion parameters[e]					
Mean frame-wise displacement, mm[f]	0.149 (0.053)	0.127 (0.079)	0.133 (0.056)	$F = 0.66$; $p = 0.521$	–
No. of frame-wise displacements >0.5 mm[g]	13.22 (10.59)	13.3 (19.60)	12.56 (14.91)	$F = 0.02$; $p = 0.978$	–
Mean root mean square[h]	0.171 (0.072)	0.187 (0.057)	0.179 (0.072)	$F = 0.257$; $p = 0.774$	–

Data are given as mean (standard deviation) unless otherwise indicated.

ASD, Autism spectrum disorder; TD, typically developing; IQ, intelligence quotient; Brother, unaffected brother.

[a] Calculated based on the diagnostic algorithm.

[b] Only 19 male youths with ASD, 19 unaffected brothers and 54 TD males had been assessed by the Chinese Social Responsiveness Scale.

[c] Only 19 male youths with ASD, 19 unaffected brothers and 41 TD males had been assessed by the Chinese Social Communication Questionnaire.

[d] Only 17 male youths with ASD, 16 unaffected brothers and 41 TD males had been assessed by the Chinese Autism Spectrum Quotient.

[e] A total of 18 male youths with ASD, 20 unaffected brothers and 48 TD males were included in the final analysis of resting-state functional magnetic imaging data.

[f] Frame-wise displacement (volume to volume displacement) was derived from Jenkinson *et al.* (2002).

[g] There were 175 available time points (volumes) for every participant, and 10 displacements correspond to 5.7% of total time points; this parameter was estimated based on Power *et al.* (2012).

[h] This parameter was estimated based on Power *et al.* (2012).

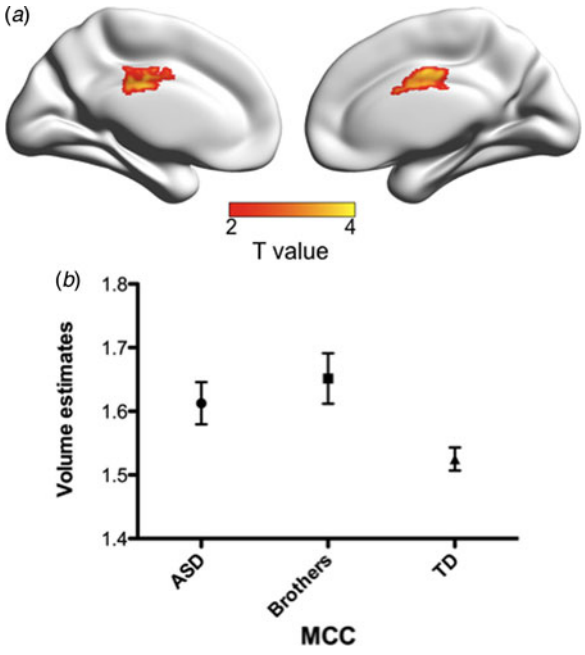

Fig. 1. Increased gray matter volume in the midcingulate cortex (MCC) is shared by male youths with autism spectrum disorder (ASD) and their unaffected brothers (Brothers). (*a*) The significant MCC cluster. (*b*) Mean volume estimates according to group. Bars represent the standard errors of the mean. TD, Typically developing males.

$p = 0.351$; WM: $F_{2,89} = 1.55$, $p = 0.218$; total brain volume: $F_{2,89} = 1.28$, $p = 0.284$) (online Supplementary Table S2).

Whole-brain conjunction analysis showed a GM cluster at the MCC (cluster surviving at FWE $p = 0.004$; MNI $x = 6$, $y = -7$, $z = 36$; BA 24/23; cluster size 2841.75 mm^3) (Fig. 1, online Supplementary Table S3). Group comparisons based on analysis of variance on the regional volume estimates extracted from this cluster revealed that both ASD probands and brothers had increased GM volume than TD (online Supplementary Table S4), suggesting that an atypical increase in GM volume in the MCC was shared by both ASD probands and their brothers.

Whole-brain conjunction analysis revealed a WM cluster located at the left superior corona radiata (cluster-level FWE corrected $p = 0.016$; MNI $x = -12$, $y = 9$, $z = 36$; cluster size 1532.25 mm^3) (Fig. 2, online Supplementary Table S3). Group comparisons from the analysis of variance on extracted volume estimates revealed that brothers and ASD probands had significantly increased WM volume than TD (online Supplementary Table S4). Subsidiary conjunction analyses from a general linear model without covarying FSIQ identified MCC (online Supplementary Fig. S1*a*) and left superior corona radiata (online Supplementary Fig. S1*b*) clusters of similar spatial extents as those identified by the main analyses.

We identified three significant clusters of iFC surviving cluster-level FWE correction at $p < 0.05$ from the conjunction analysis (Fig. 3*b* and *c*, online Supplementary Table S5). Two clusters were in the occipital cortex, with peak voxels centered at the left middle occipital gyrus (L-MoG) and right MoG (R-MoG) (Fig. 3*b*). Another cluster was at the right inferior frontal gyrus (R-IFG, Fig. 3*c*). Group comparisons based on the analysis of variance of the iFC extracted from the L-MoG revealed that ASD probands and brothers had significantly increased iFC between the L-MoG and MCC than TD (online Supplementary Table S4). Similar results were found in the R-MoG showing that both ASD and brother groups had significantly increased R-MoG-MCC iFC than TD. Group comparisons revealed significantly reduced R-IFG–MCC iFC in ASD and brothers than TD. A subsidiary general linear model without covarying FSIQ also identified bilateral MoG (online Supplementary Fig. S1*c*) and R-IFG (online Supplementary Fig. S1*d*) clusters that survived conjunction analysis. These identified clusters mentioned above demonstrated similar spatial extents to those identified by the main analyses.

Tests on familiality showed the variance of the within-pair difference of the GM volume increase in the MCC (permutation test, $p = 0.031$) and of the WM volume increase in the left superior corona radiata (permutation test, $p = 0.027$) were both smaller in biological siblings than in randomly paired pseudo-siblings, indicating that this atypicality is shared between members within the same family. By contrast, the increased iFC between the MCC and L-MOG (permutation test, $p = 0.797$) alongside R-MOG (permutation test, $p = 0.170$), and the reduced MCC-R-IFG connectivity (permutation test, $p = 0.124$) in the sib-pairs did not survive the test of familiality.

Brain–behavior relationships

As shown in online Supplementary Table S6 and Fig. 4, in the ASD group, autistic symptoms positively correlated with WM volume in the left superior corona radiata ($r = 0.644$, uncorrected $p = 0.007$), but not with other brain measures. In TD males, autistic symptoms negatively correlated with iFC between the MCC and bilateral MoG (MCC–L-MoG: $r = -0.382$, uncorrected $p = 0.016$; MCC–R-MoG: $r = -0.352$, uncorrected $p = 0.028$).

Discussion

This study is the first to use a combined structural and functional imaging approach to examine shared atypicalities in brain structures and associated iFC in youth with ASD and their unaffected siblings. With conjunction analysis we identified that male youth with ASD

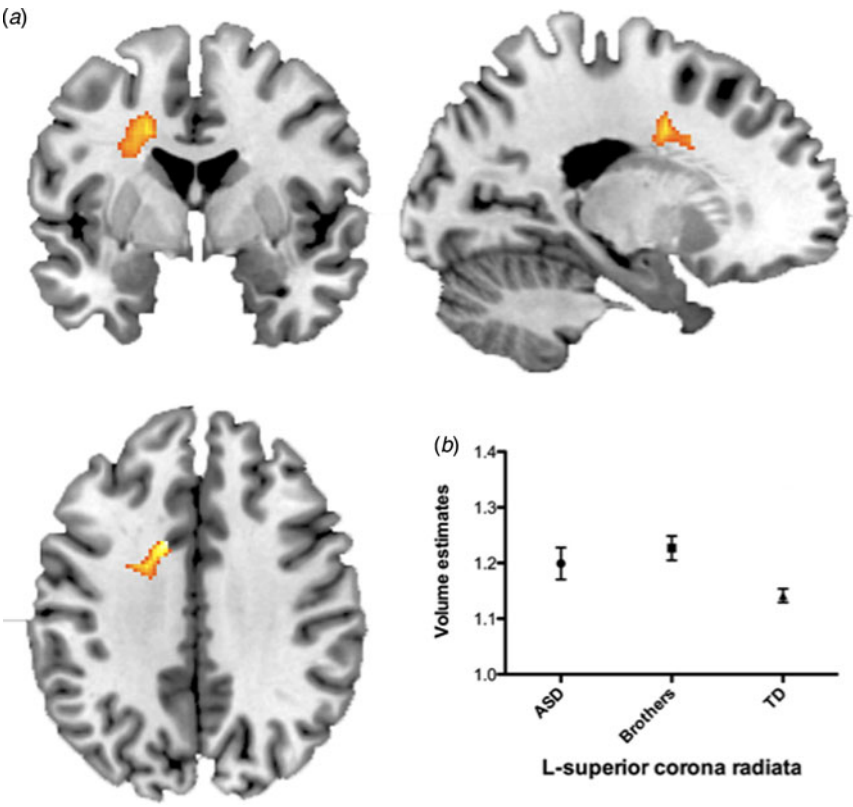

Fig. 2. Significant cluster (conjoined analyses) of increased white matter volume in the left (L) superior corona radiata in autism spectrum disorder (ASD) and unaffected brothers (Brothers) as compared with typically developing (TD) males. (*a*) The significant midcingulate cortex (MCC) cluster. (*b*) Mean volume estimates according to 'group'. Bars represent the standard errors of the mean.

and their unaffected brothers share atypically increased GM volume in the MCC, and this finding was confirmed by the test of familiality to be shared between members of the same family. MCC dysconnectivity (reduced MCC–R-IFG and increased bilateral MoG–MCC functional connectivity) were also identified by the conjunction analysis. Nonetheless, the shared iFC differences between ASD and brothers did not survive the permutation test of familiality, suggesting that other, unknown non-familial factors might also partly account for this abnormality. Our results demonstrate that unaffected brothers of ASD probands, while not behaviorally expressing ASD features, share similar neuroanatomical and neurofunctional atypicalities with their brothers with ASD.

The shared differences of GM volume among individuals with ASD and their brothers involved the MCC. This cluster lies approximately at the junction of the anterior and posterior MCC (Vogt, 2009). In TD individuals, the anterior portion of the cluster is involved in perceiving others in pain and direct experience of pain (Lamm *et al.* 2011; Shackman *et al.* 2011) and processing of negative affects (Shackman *et al.* 2011); the posterior subdivision of this region is implicated in action control (Morecraft & Tanji, 2009). Difficulty in recognition of negative emotions (Uljarevic & Hamilton, 2013), unusual embodied empathy (Hadjikhani *et al.* 2014) and a failure of empathetic behavior (Minio-Paluello *et al.* 2009) during pain observation, alongside prominent motor impairments (Dziuk *et al.* 2007) have all been reported in individuals with ASD, despite no atypical hemodynamic responses in the MCC in ASD during the motor- and affect-processing tasks (Harms *et al.* 2010; Philip *et al.* 2012). Prior functional neuroimaging findings have also revealed unusual reductions in brain activity of the MCC when individuals with autism make investment in a trust game (Chiu *et al.* 2008), view physical (Fan *et al.* 2014) and social (Krach *et al.* 2015) pain, observe hand actions (Marsh & Hamilton, 2011), and practise a working memory task (Urbain *et al.* 2015). The involvement of the MCC might be partly explained by the prior neuropathological findings of increased pyramidal neuron and von Economo neuron numbers in this region in children with autism (Uppal *et al.* 2014). Importantly, we observed that increased MCC

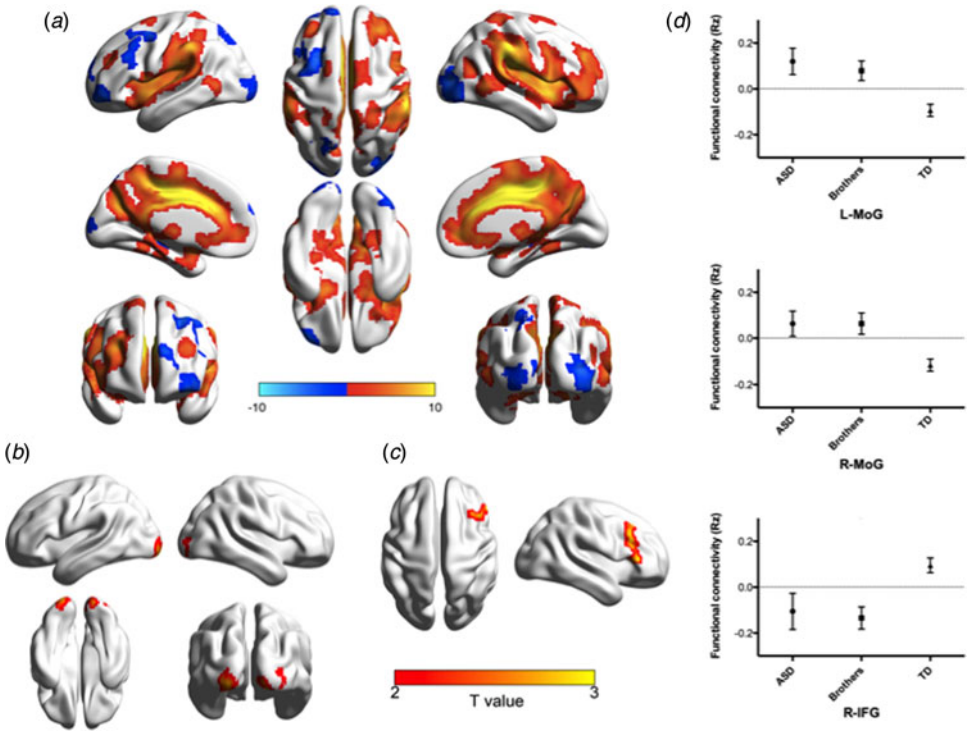

Fig. 3. Intrinsic functional connectivity based on the midcingulate cortex cluster. (*a*) Within-group functional connectivity map of typically developing (TD) male youths. (*b*) Significant clusters of shared increases in connectivity between the midcingulate cortex and bilateral middle occipital gyrus (MoG) among male youth with autism spectrum disorder (ASD) and unaffected brothers (Brothers). (*c*) A significant cluster of shared decreases in connectivity between the midcingulate cortex and right inferior frontal gyrus (R-IFG) among ASD and Brothers. (*d*) Mean functional connectivity according to group. Bars represent the standard errors of the mean. Rz, *z*-Transformed correlation coefficient; L, left; R, right.

volume was shared among ASD probands and their brothers, suggesting that this atypicality is at least partly mediated by factors common to both groups.

Based on this atypical MCC cluster, the ASD group showed reduced iFC between the R-IFG and MCC, and increased MCC–bilateral MoG connections, and, importantly, these abnormalities were also identified in their unaffected brothers. A recent meta-analysis suggests that, in TD adults, the MCC pivotally co-activates with the R-IFG in the supervisory attentional system (Cieslik *et al.* 2015). Based on the peak coordinates of this identified cluster, the functional connectivity map derived from NeuroSynth (Yarkoni *et al.* 2011) reveals that, in the TD population, the MCC is connected with the IFG, whereas no synchronous activity between the MCC and MoG is identified (thresholded at *z*-transformed $r > 0.2$). This converging evidence suggests a possible pattern of 'dysconnected' iFC in ASD, i.e. increased functional connectivity between areas that are not typically connected (Di Martino *et al.* 2011; Chien *et al.* 2015). Importantly, this dysconnectivity based on the MCC identified by the combined structural and functional MRI approach, shared among male youth with ASD and unaffected brothers, may serve as a neural vulnerability marker for ASD. Our cross-modal MRI approach could extend bidirectional structural–functional implications, which have frequently been overlooked in prior MRI literature in ASD (Mueller *et al.* 2013). Convergent findings from different modals of MRI studies may serve the field for theory validations and hypothesis generation.

Our findings correspond to the concept that brain volume (Giedd *et al.* 2010; Blokland *et al.* 2012; Hibar *et al.* 2015) and iFC (Glahn *et al.* 2010; Fornito *et al.* 2011) are largely genetically determined. Our novel finding of shared atypicality in the MCC has not been identified in prior literature on the first-degree relatives of ASD (Rojas *et al.* 2004; Palmen *et al.* 2005; Peterson *et al.* 2006; Dalton *et al.* 2007; Branchini *et al.* 2009; Segovia *et al.* 2014; Moseley *et al.* 2015). These discrepancies may arise from the following methodological considerations. First, variation in the ages of participants could modulate cortical morphometry in ASD (Nickl-Jockschat *et al.* 2012; Ecker *et al.* 2015; Lin *et al.* 2015). Some prior papers on broader autism neuroendophenotypes studied adult participants (unaffected parents) (Rojas *et al.* 2004; Palmen *et al.* 2005; Peterson *et al.* 2006), whereas

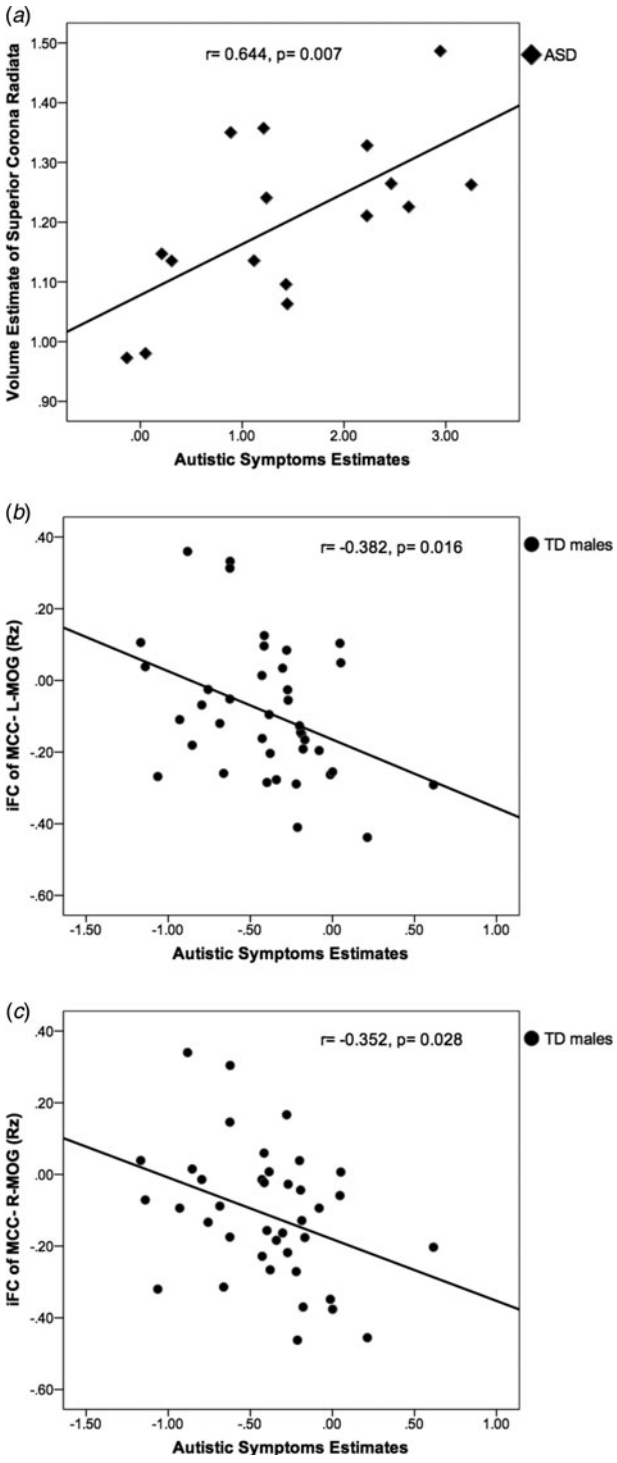

Fig. 4. Scatterplots of brain–behavior correlations. Significant correlations of (*a*) white matter volume of the left superior corona radiata with the level of autistic symptoms in male youths with autism spectrum disorder (ASD); significant correlations of intrinsic functional connectivity (iFC) between the midcingulate cortex (MCC) and (*b*) left middle occipital gyrus (L-MoG), alongside (*c*) right MoG (R-MoG), with the level of autistic symptoms in typically developing (TD) male youths. *p* Values are uncorrected. Rz, *z*-Transformed correlation coefficient.

others investigated adolescent cohorts (Dalton *et al.* 2007; Branchini *et al.* 2009; Segovia *et al.* 2014; Moseley *et al.* 2015). Here we studied youth aged 8–19 years. Although we did not identify significant age-related changes or age × group interactions, the effects of development on neuroendophenotypes for ASD awaits explorations. Furthermore, this study was limited by a lack of measure of puberty status, of which effects on brain structures and functions of ASD remain elusive. Second, only the present study and one previous work (Moseley *et al.* 2015) studied male-only participants, possibly explaining the discrepancy between our work and earlier literature using mixed-sex samples, as sex modulates brain structures in ASD (Lai *et al.* 2013, 2015; Schaer *et al.* 2015; Supekar & Menon, 2015). Another critical issue is the selection of participants based on the familial occurrence of ASD. In the present study, we recruited simplex families. However, previous studies on neuroendophenotypes or broader autism neurophenotypes allow for samples of unaffected first-degree relatives to be from either families with only one individual with ASD (simplex families), or families with two or more affected individuals (multiplex families). The current sample of simplex families might partly contribute to disparity between findings of prior studies on siblings of ASD and ours. Finally, the different genetic (Kuo et al. 2015; Liu *et al.* 2015) or cultural (Han & Ma, 2015) backgrounds of the samples may also contribute to the discrepant reports.

To facilitate endophenotype discovery, we adopted a three-group (i.e. ASD, unaffected relatives, TD controls) (Dalton *et al.* 2007; Segovia *et al.* 2014; Moseley *et al.* 2015), rather than a two-group (i.e. unaffected relatives and healthy controls) (Rojas *et al.* 2004; Palmen *et al.* 2005; Peterson *et al.* 2006; Branchini *et al.* 2009), design. Statistically, inclusion of three groups within a general linear model with conjunction analyses may partly explain our distinct but limited finding in the MCC differences. However, we assert that more precise neuroendophenotypic markers for ASD could be identified by adopting these approaches in the current study (Kaiser *et al.* 2010). This design specifies 'trait' signature, i.e. shared atypicality in siblings and autistic probands, and partly explains the distinct findings between the current study ('trait' features) (Kaiser *et al.* 2010), literature on ASD probands alone, and siblings alone. Notably, the significant conjunction that we identified does not indicate that all the contrasts were individually significant (i.e. a conjunction of significance). It simply means that the contrasts were consistently high and jointly significant (Friston *et al.* 2005). This account highlights the unique interpretations using the conjunction analyses (Friston *et al.* 2005; Heller *et al.* 2007), which is not the common

approach in the earlier neuroimaging literature on ASD relatives. Moreover, despite the advantage of the current design, it should be noted that we did not employ a linear mixed-effects model, a suggested approach for accounting for relatedness and heritability among subjects within the families (Chen *et al.* 2013), as the current neuroimaging software has difficulty handling the conjunction analysis for this complex model. Alternatively, we tested the variance of the within-family-pair difference as an assessment of familiality (Menzies *et al.* 2007; Ersche *et al.* 2012) to aid interpretation of the findings from fixed-effect models. Finally, despite the sophisticated study designs, the current findings are still limited by the relatively modest sample size in the ASD and brother groups, and should be further replicated in a large-scale independent cohort.

With regard to imaging methodology, as in-scanner head motion would introduce artifacts in both structural (Reuter *et al.* 2015) and functional image (Power *et al.* 2015), we used stringent motion-exclusion criteria, a robust motion-denoising strategy (i.e. ICA-AROMA), matching motion composite across groups, and including mean FD as a covariate in the statistical models for rs-fMRI data (Yan *et al.* 2013*a*). Nonetheless, we acknowledge that even a relatively small amount of head motion may still confound the present findings. Herein, we adopted the VBM approach to identify structural differences, which may be sensitive to the inaccuracy of tissue-classification and smoothing extents (Mechelli *et al.* 2005). To date, no study on unaffected relatives of ASD has applied surface-based morphometry. Future studies could adopt both voxel-based and surface-based methods to complement each other. Lastly, although we employed seed-based correlation analysis to directly link structural anomalies to iFC, interpreting these resulting spatial map and group difference as the sole finding is an under-representation of the data, as only one network is tested. Different seed-selection strategies may bias the reports (Cole *et al.* 2010). Future work using a more refined approach to integrate structural and functional features, which balance the unbiased data-driven explorations and hypothesis-based selections of the candidate systems in the contexts of overall literature of ASD, is warranted.

In summary, using a combined structural MRI and rs-fMRI approach, we reported for the first time that increased GM volume in the MCC and its dysconnected iFC were shared among male youth with ASD and their unaffected brothers. This highlights that the MCC may be a candidate neuroendophenotype for ASD. Our findings characterized the underlying trait of vulnerability to develop ASD in light of the structures and functions of the MCC. This might have implications for discovering factors common to both affected individuals and unaffected relatives, which give rise to atypical neuroanatomy and brain connections.

Supplementary material

The supplementary material for this article can be found at https://doi.org/10.1017/S0033291716002695

Acknowledgements

This work was supported by grants from the National Science Council of Taiwan (NSC 97-3112-B-002-009, NSC98-3112-B-002-004, NSC 99-2627-B-002-015, NSC 100-2627-B-002-014, NSC 101-2627-B-002-002, NSC 101-2314-B-002-136-MY3), National Taiwan University (AIM for Top University Excellent Research Project: 10R81918-03, 101R892103, 102R892103), and the National Taiwan University Hospital (NTUH101-S1910, NTUH103-N2574, NTUH104-S2761). M.-C.L. is supported by the O'Brien Scholars Program within the Child and Youth Mental Health Collaborative at the Centre for Addiction and Mental Health and The Hospital for Sick Children, Toronto. We are grateful for all participants and their parents for taking part in the study.

S.S.-F.G. was the principal investigator of this study. H.-Y.L and S.S.-F.G. were responsible for the study concept and design. S.S.-F.G. recruited and assessed participants and acquired clinical data. S.S.-F.G. and W.-Y.I.T. supervised the study and acquired imaging data. H.-Y.L., S.S.-F.G. and Y.-T.C. analysed and interpreted the data. H.-Y.L. produced the figures. H.-Y.L., M.-C.L. and S.S.-F.G. wrote the manuscript. All authors read and approved the manuscript.

Declaration of Interest

None.

References

Amaral DG, Schumann CM, Nordahl CW (2008). Neuroanatomy of autism. *Trends in Neurosciences* **31**, 137–145.

Ashburner J (2007). A fast diffeomorphic image registration algorithm. *NeuroImage* **38**, 95–113.

Baron-Cohen S, Wheelwright S, Skinner R, Martin J, Clubley E (2001). The Autism-Spectrum Quotient (AQ): evidence from Asperger syndrome/high-functioning autism, males and females, scientists and mathematicians. *Journal of Autism and Developmental Disorders* **31**, 5–17.

Behzadi Y, Restom K, Liau J, Liu TT (2007). A component based noise correction method (CompCor) for BOLD and perfusion based fMRI. *NeuroImage* **37**, 90–101.

Belmonte MK, Allen G, Beckel-Mitchener A, Boulanger LM, Carper RA, Webb SJ (2004). Autism and abnormal development of brain connectivity. *Journal of Neuroscience* **24**, 9228–9231.

Belton E, Salmond CH, Watkins KE, Vargha-Khadem F, Gadian DG (2003). Bilateral brain abnormalities associated with dominantly inherited verbal and orofacial dyspraxia. *Human Brain Mapping* **18**, 194–200.

Blokland GA, de Zubicaray GI, McMahon KL, Wright MJ (2012). Genetic and environmental influences on neuroimaging phenotypes: a meta-analytical perspective on twin imaging studies. *Twin Research and Human Genetics: the Official Journal of the International Society for Twin Studies* **15**, 351–371.

Branchini LA, Lindgren KA, Tager-Flusberg H (2009). MRI analysis of the corpus callosum in siblings of children with autism spectrum disorder. *Neurology* **72**, A136–A136.

Chen G, Saad ZS, Britton JC, Pine DS, Cox RW (2013). Linear mixed-effects modeling approach to fMRI group analysis. *NeuroImage* **73**, 176–190.

Chien HY, Lin HY, Lai MC, Gau SS, Tseng WY (2015). Hyperconnectivity of the right posterior temporo-parietal junction predicts social difficulties in boys with autism spectrum disorder. *Autism Research* **8**, 427–441.

Chiu PH, Kayali MA, Kishida KT, Tomlin D, Klinger LG, Klinger MR, Montague PR (2008). Self responses along cingulate cortex reveal quantitative neural phenotype for high-functioning autism. *Neuron* **57**, 463–473.

Cieslik EC, Mueller VI, Eickhoff CR, Langner R, Eickhoff SB (2015). Three key regions for supervisory attentional control: evidence from neuroimaging meta-analyses. *Neuroscience and Biobehavioral Reviews* **48**, 22–34.

Cole DM, Smith SM, Beckmann CF (2010). Advances and pitfalls in the analysis and interpretation of resting-state fMRI data. *Frontiers in Systems Neuroscience* **4**, 8.

Colvert E, Tick B, McEwen F, Stewart C, Curran SR, Woodhouse E, Gillan N, Hallett V, Lietz S, Garnett T, Ronald A, Plomin R, Rijsdijk F, Happe F, Bolton P (2015). Heritability of autism spectrum disorder in a UK population-based twin sample. *JAMA Psychiatry* **72**, 415–423.

Courchesne E, Pierce K, Schumann CM, Redcay E, Buckwalter JA, Kennedy DP, Morgan J (2007). Mapping early brain development in autism. *Neuron* **56**, 399–413.

D'Mello AM, Crocetti D, Mostofsky SH, Stoodley CJ (2015). Cerebellar gray matter and lobular volumes correlate with core autism symptoms. *NeuroImage: Clinical* **7**, 631–639.

Dalton KM, Nacewicz BM, Alexander AL, Davidson RJ (2007). Gaze-fixation, brain activation, and amygdala volume in unaffected siblings of individuals with autism. *Biological Psychiatry* **61**, 512–520.

Di Martino A, Kelly C, Grzadzinski R, Zuo XN, Mennes M, Mairena MA, Lord C, Castellanos FX, Milham MP (2011). Aberrant striatal functional connectivity in children with autism. *Biological Psychiatry* **69**, 847–856.

Di Martino A, Yan CG, Li Q, Denio E, Castellanos FX, Alaerts K, Anderson JS, Assaf M, Bookheimer SY, Dapretto M, Deen B, Delmonte S, Dinstein I, Ertl-Wagner B, Fair DA, Gallagher L, Kennedy DP, Keown CL, Keysers C, Lainhart JE, Lord C, Luna B, Menon V, Minshew NJ, Monk CS, Mueller S, Müller RA, Nebel MB, Nigg JT, O'Hearn K, Pelphrey KA, Peltier SJ, Rudie JD, Sunaert S, Thioux M, Tyszka JM, Uddin LQ, Verhoeven JS, Wenderoth N, Wiggins JL, Mostofsky SH, Milham MP (2014). The autism brain imaging data exchange: towards a large-scale evaluation of the intrinsic brain architecture in autism. *Molecular Psychiatry* **19**, 659–667.

Dziuk MA, Gidley Larson JC, Apostu A, Mahone EM, Denckla MB, Mostofsky SH (2007). Dyspraxia in autism: association with motor, social, and communicative deficits. *Developmental Medicine and Child Neurology* **49**, 734–739.

Ecker C, Bookheimer SY, Murphy DG (2015). Neuroimaging in autism spectrum disorder: brain structure and function across the lifespan. *Lancet Neurology* **14**, 1121–1134.

Ersche KD, Jones PS, Williams GB, Turton AJ, Robbins TW, Bullmore ET (2012). Abnormal brain structure implicated in stimulant drug addiction. *Science* **335**, 601–604.

Fan YT, Chen C, Chen SC, Decety J, Cheng Y (2014). Empathic arousal and social understanding in individuals with autism: evidence from fMRI and ERP measurements. *Social Cognitive and Affective Neuroscience* **9**, 1203–1213.

Fishman I, Keown CL, Lincoln AJ, Pineda JA, Müller RA (2014). Atypical cross talk between mentalizing and mirror neuron networks in autism spectrum disorder. *JAMA Psychiatry* **71**, 751–760.

Fornito A, Zalesky A, Bassett DS, Meunier D, Ellison-Wright I, Yucel M, Wood SJ, Shaw K, O'Connor J, Nertney D, Mowry BJ, Pantelis C, Bullmore ET (2011). Genetic influences on cost-efficient organization of human cortical functional networks. *Journal of Neuroscience* **31**, 3261–3270.

Friston KJ, Holmes AP, Price CJ, Buchel C, Worsley KJ (1999). Multisubject fMRI studies and conjunction analyses. *NeuroImage* **10**, 385–396.

Friston KJ, Penny WD, Glaser DE (2005). Conjunction revisited. *NeuroImage* **25**, 661–667.

Gau SS, Chong MY, Chen TH, Cheng AT (2005). A 3-year panel study of mental disorders among adolescents in Taiwan. *American Journal of Psychiatry* **162**, 1344–1350.

Gau SSF, Chou MC, Lee JC, Wong CC, Chou WJ, Chen MF, Soong WT, Wu YY (2010). Behavioral problems and parenting style among Taiwanese children with autism and their siblings. *Psychiatry and Clinical Neurosciences* **64**, 70–78.

Gau SS-F, Lee C-M, Lai M-C, Chiu Y-N, Huang Y-F, Kao J-D, Wu Y-Y (2011). Psychometric properties of the Chinese version of the Social Communication Questionnaire. *Research in Autism Spectrum Disorders* **5**, 809–818.

Gau SS-F, Liu L-T, Wu Y-Y, Chiu Y-N, Tsai W-C (2013). Psychometric properties of the Chinese version of the Social Responsiveness Scale. *Research in Autism Spectrum Disorders* **7**, 349–360.

Geschwind DH, State MW (2015). Gene hunting in autism spectrum disorder: on the path to precision medicine. *Lancet Neurology* **14**, 1109–1120.

Giedd JN, Stockman M, Weddle C, Liverpool M, Alexander-Bloch A, Wallace GL, Lee NR, Lalonde F, Lenroot RK (2010). Anatomic magnetic resonance imaging of the

developing child and adolescent brain and effects of genetic variation. *Neuropsychology Review* **20**, 349–361.

Glahn DC, Knowles EE, McKay DR, Sprooten E, Raventos H, Blangero J, Gottesman II, Almasy L (2014). Arguments for the sake of endophenotypes: examining common misconceptions about the use of endophenotypes in psychiatric genetics. *American Journal of Medical Genetics. Part B, Neuropsychiatric Genetics* **165B**, 122–130.

Glahn DC, Winkler AM, Kochunov P, Almasy L, Duggirala R, Carless MA, Curran JC, Olvera RL, Laird AR, Smith SM, Beckmann CF, Fox PT, Blangero J (2010). Genetic control over the resting brain. *Proceedings of the National Academy of Sciences USA* **107**, 1223–1228.

Gottesman II, Gould TD (2003). The endophenotype concept in psychiatry: etymology and strategic intentions. *American Journal of Psychiatry* **160**, 636–645.

Hadjikhani N, Zurcher NR, Rogier O, Hippolyte L, Lemonnier E, Ruest T, Ward N, Lassalle A, Gillberg N, Billstedt E, Helles A, Gillberg C, Solomon P, Prkachin KM, Gillberg C (2014). Emotional contagion for pain is intact in autism spectrum disorders. *Translational Psychiatry* **4**, e343.

Hallquist MN, Hwang K, Luna B (2013). The nuisance of nuisance regression: spectral misspecification in a common approach to resting-state fMRI preprocessing reintroduces noise and obscures functional connectivity. *NeuroImage* **82**, 208–225.

Han S, Ma Y (2015). A culture–behavior–brain loop model of human development. *Trends in Cognitive Sciences* **19**, 666–676.

Harms MB, Martin A, Wallace GL (2010). Facial emotion recognition in autism spectrum disorders: a review of behavioral and neuroimaging studies. *Neuropsychology Review* **20**, 290–322.

Hayasaka S, Nichols TE (2003). Validating cluster size inference: random field and permutation methods. *NeuroImage* **20**, 2343–2356.

Heller R, Golland Y, Malach R, Benjamini Y (2007). Conjunction group analysis: an alternative to mixed/random effect analysis. *NeuroImage* **37**, 1178–1185.

Hibar DP, Stein JL, Renteria ME, Arias-Vasquez A, Desrivières S, Jahanshad N, Toro R, Wittfeld K, Abramovic L, Andersson M, Aribisala BS, Armstrong NJ, Bernard M, Bohlken MM, Boks MP, Bralten J, Brown AA, Chakravarty MM, Chen Q, Ching CR, Cuellar-Partida G, den Braber A, Giddaluru S, Goldman AL, Grimm O, Guadalupe T, Hass J, Woldehawariat G, Holmes AJ, Hoogman M, Janowitz D, Jia T, Kim S, Klein M, Kraemer B, Lee PH, Olde Loohuis LM, Luciano M, Macare C, Mather KA, Mattheisen M, Milaneschi Y, Nho K, Papmeyer M, Ramasamy A, Risacher SL, Roiz-Santiañez R, Rose EJ, Salami A, Sämann PG, Schmaal L, Schork AJ, Shin J, Strike LT, Teumer A, van Donkelaar MM, van Eijk KR, Walters RK, Westlye LT, Whelan CD, Winkler AM, Zwiers MP, Alhusaini S, Athanasiu L, Ehrlich S, Hakobjan MM, Hartberg CB, Haukvik UK, Heister AJ, Hoehn D, Kasperaviciute D, Liewald DC, Lopez LM, Makkinje RR, Matarin M, Naber MA, McKay DR, Needham M, Nugent AC, Pütz B, Royle NA, Shen L, Sprooten E, Trabzuni D, van der Marel SS, van Hulzen KJ, Walton E, Wolf C, Almasy L, Ames D, Arepalli S, Assareh AA, Bastin ME, Brodaty H, Bulayeva KB, Carless MA, Cichon S, Corvin A, Curran JE, Czisch M, de Zubicaray GI, Dillman A, Duggirala R, Dyer TD, Erk S, Fedko IO, Ferrucci L, Foroud TM, Fox PT, Fukunaga M, Gibbs JR, Göring HH, Green RC, Guelfi S, Hansell NK, Hartman CA, Hegenscheid K, Heinz A, Hernandez DG, Heslenfeld DJ, Hoekstra PJ, Holsboer F, Homuth G, Hottenga JJ, Ikeda M, Jack Jr. CR, Jenkinson M, Johnson R, Kanai R, Keil M, Kent Jr. JW, Kochunov P, Kwok JB, Lawrie SM, Liu X, Longo DL, McMahon KL, Meisenzahl E, Melle I, Mohnke S, Montgomery GW, Mostert JC, Mühleisen TW, Nalls MA, Nichols TE, Nilsson LG, Nöthen MM, Ohi K, Olvera RL, Perez-Iglesias R, Pike GB, Potkin SG, Reinvang I, Reppermund S, Rietschel M, Romanczuk-Seiferth N, Rosen GD, Rujescu D, Schnell K, Schofield PR, Smith C, Steen VM, Sussmann JE, Thalamuthu A, Toga AW, Traynor BJ, Troncoso J, Turner JA, Valdés Hernández MC, van 't Ent D, van der Brug M, van der Wee NJ, van Tol MJ, Veltman DJ, Wassink TH, Westman E, Zielke RH, Zonderman AB, Ashbrook DG, Hager R, Lu L, McMahon FJ, Morris DW, Williams RW, Brunner HG, Buckner RL, Buitelaar JK, Cahn W, Calhoun VD, Cavalleri GL, Crespo-Facorro B, Dale AM, Davies GE, Delanty N, Depondt C, Djurovic S, Drevets WC, Espeseth T, Gollub RL, Ho BC, Hoffmann W, Hosten N, Kahn RS, Le Hellard S, Meyer-Lindenberg A, Müller-Myhsok B, Nauck M, Nyberg L, Pandolfo M, Penninx BW, Roffman JL, Sisodiya SM, Smoller JW, van Bokhoven H, van Haren NE, Völzke H, Walter H, Weiner MW, Wen W, White T, Agartz I, Andreassen OA, Blangero J, Boomsma DI, Brouwer RM, Cannon DM, Cookson MR, de Geus EJ, Deary IJ, Donohoe G, Fernández G, Fisher SE, Francks C, Glahn DC, Grabe HJ, Gruber O, Hardy J, Hashimoto R, Hulshoff Pol HE, Jönsson EG, Kloszewska I, Lovestone S, Mattay VS, Mecocci P, McDonald C, McIntosh AM, Ophoff RA, Paus T, Pausova Z, Ryten M, Sachdev PS, Saykin AJ, Simmons A, Singleton A, Soininen H, Wardlaw JM, Weale ME, Weinberger DR, Adams HH, Launer LJ, Seiler S, Schmidt R, Chauhan G, Satizabal CL, Becker JT, Yanek L, van der Lee SJ, Ebling M, Fischl B, Longstreth Jr WT, Greve D, Schmidt H, Nyquist P, Vinke LN, van Duijn CM, Xue L, Mazoyer B, Bis JC, Gudnason V, Seshadri S, Ikram MA; Alzheimer's Disease Neuroimaging Initiative; CHARGE Consortium; EPIGEN; IMAGEN; SYS, Martin NG, Wright MJ, Schumann G, Franke B, Thompson PM, Medland SE (2015). Common genetic variants influence human subcortical brain structures. *Nature* **520**, 224–229.

Hsiao MN, Tseng WL, Huang HY, Gau SS (2013). Effects of autistic traits on social and school adjustment in children and adolescents: the moderating roles of age and gender. *Research in Developmental Disabilities* **34**, 254–265.

Hua K, Zhang J, Wakana S, Jiang H, Li X, Reich DS, Calabresi PA, Pekar JJ, van Zijl PC, Mori S (2008). Tract probability maps in stereotaxic spaces: analyses of white matter anatomy and tract-specific quantification. *NeuroImage* **39**, 336–347.

Jenkinson M, Bannister P, Brady M, Smith S (2002). Improved optimization for the robust and accurate linear registration and motion correction of brain images. *NeuroImage* **17**, 825–841.

Kaiser MD, Hudac CM, Shultz S, Lee SM, Cheung C, Berken AM, Deen B, Pitskel NB, Sugrue DR, Voos AC, Saulnier CA, Ventola P, Wolf JM, Klin A, Vander Wyk BC, Pelphrey KA (2010). Neural signatures of autism. *Proceedings of the National Academy of Sciences USA* **107**, 21223–21228.

Kim YS, Leventhal BL (2015). Genetic epidemiology and insights into interactive genetic and environmental effects in autism spectrum disorders. *Biological Psychiatry* **77**, 66–74.

Krach S, Kamp-Becker I, Einhauser W, Sommer J, Frassle S, Jansen A, Rademacher L, Muller-Pinzler L, Gazzola V, Paulus FM (2015). Evidence from pupillometry and fMRI indicates reduced neural response during vicarious social pain but not physical pain in autism. *Human Brain Mapping* **36**, 4730–4744.

Kuo C-C, Liang K-C, Tseng CC, Gau SS-F (2014). Comparison of the cognitive profiles and social adjustment between mathematically and scientifically talented students and students with Asperger's syndrome. *Research in Autism Spectrum Disorders* **8**, 838–850.

Kuo PH, Chuang LC, Su MH, Chen CH, Chen CH, Wu JY, Yen CJ, Wu YY, Liu SK, Chou MC, Chou WJ, Chiu YN, Tsai WC, Gau SS (2015). Genome-wide association study for autism spectrum disorder in Taiwanese Han population. *PLOS ONE* **10**, e0138695.

Lai MC, Lombardo MV, Auyeung B, Chakrabarti B, Baron-Cohen S (2015). Sex/gender differences and autism: setting the scene for future research. *Journal of the American Academy of Child and Adolescent Psychiatry* **54**, 11–24.

Lai MC, Lombardo MV, Suckling J, Ruigrok AN, Chakrabarti B, Ecker C, Deoni SC, Craig MC, Murphy DG, Bullmore ET; MRC AIMS Consortium, Baron-Cohen S (2013). Biological sex affects the neurobiology of autism. *Brain* **136**, 2799–2815.

Lamm C, Decety J, Singer T (2011). Meta-analytic evidence for common and distinct neural networks associated with directly experienced pain and empathy for pain. *NeuroImage* **54**, 2492–2502.

Lau WY, Gau SS, Chiu YN, Wu YY (2014). Autistic traits in couple dyads as a predictor of anxiety spectrum symptoms. *Journal of Autism and Developmental Disorders* **44**, 2949–2963.

Lau WYP, Gau SSF, Chiu YN, Wu YY, Chou WJ, Liu SK, Chou MC (2013). Psychometric properties of the Chinese version of the Autism Spectrum Quotient (AQ). *Research in Developmental Disabilities* **34**, 294–305.

Lin H-Y, Ni H-C, Lai M-C, Tseng W-YI, Gau SSF (2015). Regional brain volume differences between males with and without autism spectrum disorder are highly age-dependent. *Molecular Autism* **6**, 29.

Liu X, Shimada T, Otowa T, Wu YY, Kawamura Y, Tochigi M, Iwata Y, Umekage T, Toyota T, Maekawa M, Iwayama Y, Suzuki K, Kakiuchi C, Kuwabara H, Kano Y, Nishida H, Sugiyama T, Kato N, Chen CH, Mori N, Yamada K, Yoshikawa T, Kasai K, Tokunaga K, Sasaki T, Gau SS (2016). Genome-wide association study of autism spectrum disorder in the East Asian populations. *Autism Research* **9**, 340–349.

Marsh LE, Hamilton AF (2011). Dissociation of mirroring and mentalising systems in autism. *NeuroImage* **56**, 1511–1519.

Mechelli A, Price CJ, Friston KJ, Ashburner J (2005). Voxel-based morphometry of the human brain: methods and applications. *Current Medical Imaging Reviews* **1**, 105–113.

Menzies L, Achard S, Chamberlain SR, Fineberg N, Chen CH, del Campo N, Sahakian BJ, Robbins TW, Bullmore E (2007). Neurocognitive endophenotypes of obsessive–compulsive disorder. *Brain* **130**, 3223–3236.

Minio-Paluello I, Baron-Cohen S, Avenanti A, Walsh V, Aglioti SM (2009). Absence of embodied empathy during pain observation in Asperger syndrome. *Biological Psychiatry* **65**, 55–62.

Morecraft RJ, Tanji J (2009). Cingulofrontal interactions and the cingulate motor areas. In *Cingulate Neurobiology and Disease* (ed. BA Vogt), pp. 113–144. Oxford University Press: Oxford.

Moseley RL, Ypma RJ, Holt RJ, Floris D, Chura LR, Spencer MD, Baron-Cohen S, Suckling J, Bullmore E, Rubinov M (2015). Whole-brain functional hypoconnectivity as an endophenotype of autism in adolescents. *NeuroImage: Clinical* **9**, 140–152.

Mueller S, Keeser D, Samson AC, Kirsch V, Blautzik J, Grothe M, Erat O, Hegenloh M, Coates U, Reiser MF, Hennig-Fast K, Meindl T (2013). Convergent findings of altered functional and structural brain connectivity in individuals with high functioning autism: a multimodal MRI study. *PLOS ONE* **8**, e67329.

Müller RA, Shih P, Keehn B, Deyoe JR, Leyden KM, Shukla DK (2011). Underconnected, but how? A survey of functional connectivity MRI studies in autism spectrum disorders. *Cerebral Cortex* **21**, 2233–2243.

Nickl-Jockschat T, Habel U, Michel TM, Manning J, Laird AR, Fox PT, Schneider F, Eickhoff SB (2012). Brain structure anomalies in autism spectrum disorder – a meta-analysis of VBM studies using anatomic likelihood estimation. *Human Brain Mapping* **33**, 1470–1489.

Oldfield RC (1971). The assessment and analysis of handedness: the Edinburgh Inventory. *Neuropsychologia* **9**, 97–113.

Palmen SJ, Hulshoff Pol HE, Kemner C, Schnack HG, Sitskoorn MM, Appels MC, Kahn RS, Van Engeland H (2005). Brain anatomy in non-affected parents of autistic probands: a MRI study. *Psychological Medicine* **35**, 1411–1420.

Peterson E, Schmidt GL, Tregellas JR, Winterrowd E, Kopelioff L, Hepburn S, Reite M, Rojas DC (2006). A voxel-based morphometry study of gray matter in parents of children with autism. *Neuroreport* **17**, 1289–1292.

Philip RC, Dauvermann MR, Whalley HC, Baynham K, Lawrie SM, Stanfield AC (2012). A systematic review and meta-analysis of the fMRI investigation of autism spectrum disorders. *Neuroscience and Biobehavioral Reviews* **36**, 901–942.

Pironti VA, Lai MC, Muller U, Dodds CM, Suckling J, Bullmore ET, Sahakian BJ (2014). Neuroanatomical

abnormalities and cognitive impairments are shared by adults with attention-deficit/hyperactivity disorder and their unaffected first-degree relatives. *Biological Psychiatry* **76**, 639–647.

Power JD, Barnes KA, Snyder AZ, Schlaggar BL, Petersen SE (2012). Spurious but systematic correlations in functional connectivity MRI networks arise from subject motion. *NeuroImage* **59**, 2142–2154.

Power JD, Schlaggar BL, Petersen SE (2015). Recent progress and outstanding issues in motion correction in resting state fMRI. *NeuroImage* **105**, 536–551.

Pruim RH, Mennes M, Buitelaar JK, Beckmann CF (2015*a*). Evaluation of ICA-AROMA and alternative strategies for motion artifact removal in resting state fMRI. *NeuroImage* **112**, 278–287.

Pruim RH, Mennes M, van Rooij D, Llera A, Buitelaar JK, Beckmann CF (2015*b*). ICA-AROMA: a robust ICA-based strategy for removing motion artifacts from fMRI data. *NeuroImage* **112**, 267–277.

Reuter M, Tisdall MD, Qureshi A, Buckner RL, van der Kouwe AJ, Fischl B (2015). Head motion during MRI acquisition reduces gray matter volume and thickness estimates. *NeuroImage* **107**, 107–115.

Rojas DC, Smith JA, Benkers TL, Camou SL, Reite ML, Rogers SJ (2004). Hippocampus and amygdala volumes in parents of children with autistic disorder. *American Journal of Psychiatry* **161**, 2038–2044.

Rorden C, Karnath HO, Bonilha L (2007). Improving lesion–symptom mapping. *Journal of Cognitive Neuroscience* **19**, 1081–1088.

Rutter M, Le Couteur A, Lord C (2003). *Autism Diagnostic Interview-Revised*. Western Psychological Services: Los Angeles, CA.

Sandin S, Lichtenstein P, Kuja-Halkola R, Larsson H, Hultman CM, Reichenberg A (2014). The familial risk of autism. *JAMA* **311**, 1770–1777.

Schaer M, Kochalka J, Padmanabhan A, Supekar K, Menon V (2015). Sex differences in cortical volume and gyrification in autism. *Molecular Autism* **6**, 42.

Schipul SE, Keller TA, Just MA (2011). Inter-regional brain communication and its disturbance in autism. *Frontiers in Systems Neuroscience* **5**, 10.

Segovia F, Holt R, Spencer M, Gorriz JM, Ramirez J, Puntonet CG, Phillips C, Chura L, Baron-Cohen S, Suckling J (2014). Identifying endophenotypes of autism: a multivariate approach. *Frontiers in Computational Neuroscience* **8**, 60.

Shackman AJ, Salomons TV, Slagter HA, Fox AS, Winter JJ, Davidson RJ (2011). The integration of negative affect, pain and cognitive control in the cingulate cortex. *Nature Reviews Neuroscience* **12**, 154–167.

Song XW, Dong ZY, Long XY, Li SF, Zuo XN, Zhu CZ, He Y, Yan CG, Zang YF (2011). REST: a toolkit for resting-state functional magnetic resonance imaging data processing. *PLoS ONE* **6**, e25031.

Spencer MD, Chura LR, Holt RJ, Suckling J, Calder AJ, Bullmore ET, Baron-Cohen S (2012). Failure to deactivate the default mode network indicates a possible endophenotype of autism. *Molecular Autism* **3**, 15.

Suckling J (2011). Correlated covariates in ANCOVA cannot adjust for pre-existing differences between groups. *Schizophrenia Research* **126**, 310–311.

Sucksmith E, Roth I, Hoekstra RA (2011). Autistic traits below the clinical threshold: re-examining the broader autism phenotype in the 21st century. *Neuropsychology Review* **21**, 360–389.

Supekar K, Menon V (2015). Sex differences in structural organization of motor systems and their dissociable links with repetitive/restricted behaviors in children with autism. *Molecular Autism* **6**, 50.

Tzourio-Mazoyer N, Landeau B, Papathanassiou D, Crivello F, Etard O, Delcroix N, Mazoyer B, Joliot M (2002). Automated anatomical labeling of activations in SPM using a macroscopic anatomical parcellation of the MNI MRI single-subject brain. *NeuroImage* **15**, 273–289.

Uddin LQ, Supekar K, Menon V (2013). Reconceptualizing functional brain connectivity in autism from a developmental perspective. *Frontiers in Human Neuroscience* **7**, 458.

Uljarevic M, Hamilton A (2013). Recognition of emotions in autism: a formal meta-analysis. *Journal of Autism and Developmental Disorders* **43**, 1517–1526.

Uppal N, Wicinski B, Buxbaum JD, Heinsen H, Schmitz C, Hof PR (2014). Neuropathology of the anterior midcingulate cortex in young children with autism. *Journal of Neuropathology and Experimental Neurology* **73**, 891–902.

Urbain CM, Pang EW, Taylor MJ (2015). Atypical spatiotemporal signatures of working memory brain processes in autism. *Translational Psychiatry* **5**, e617.

Van Dijk KR, Hedden T, Venkataraman A, Evans KC, Lazar SW, Buckner RL (2010). Intrinsic functional connectivity as a tool for human connectomics: theory, properties, and optimization. *Journal of Neurophysiology* **103**, 297–321.

Vissers ME, Cohen MX, Geurts HM (2012). Brain connectivity and high functioning autism: a promising path of research that needs refined models, methodological convergence, and stronger behavioral links. *Neuroscience and Biobehavioral Reviews* **36**, 604–625.

Vogt BA (2009). Regions and subregions of the cingulate cortex. In *Cingulate Neurobiology and Disease* (ed. BA Vogt), pp. 3–30. Oxford University Press: Oxford.

Wakana S, Caprihan A, Panzenboeck MM, Fallon JH, Perry M, Gollub RL, Hua K, Zhang J, Jiang H, Dubey P, Blitz A, van Zijl P, Mori S (2007). Reproducibility of quantitative tractography methods applied to cerebral white matter. *NeuroImage* **36**, 630–644.

Wass S (2011). Distortions and disconnections: disrupted brain connectivity in autism. *Brain and Cognition* **75**, 18–28.

Wechsler D (1991). *Wechsler Intelligence Scale for Children – Third Edition* (*WISC-III*). Psychological Corporation: San Antonio, TX.

Wechsler D (1997). *Wechsler Adult Intelligence Scale – Third Edition (WAIS-III)*. Psychological Corporation: San Antonio, TX.

Whitfield-Gabrieli S, Nieto-Castanon A (2012). Conn: a functional connectivity toolbox for correlated and anticorrelated brain networks. *Brain Connectivity* **2**, 125–141.

Wilke M, Holland SK, Altaye M, Gaser C (2008). Template-O-Matic: a toolbox for creating customized pediatric templates. *NeuroImage* **41**, 903–913.

Xia M, Wang J, He Y (2013). BrainNet Viewer: a network visualization tool for human brain connectomics. *PLOS ONE* **8**, e68910.

Yan CG, Cheung B, Kelly C, Colcombe S, Craddock RC, Di Martino A, Li Q, Zuo XN, Castellanos FX, Milham MP (2013*a*). A comprehensive assessment of regional variation in the impact of head micromovements on functional connectomics. *NeuroImage* **76**, 183–201.

Yan CG, Craddock RC, Zuo XN, Zang YF, Milham MP (2013*b*). Standardizing the intrinsic brain: towards robust measurement of inter-individual variation in 1000 functional connectomes. *NeuroImage* **80**, 246–262.

Yan CG, Zang YF (2010). DPARSF: a MATLAB toolbox for "Pipeline" data analysis of resting-state fMRI. *Frontiers in Systems Neuroscience* **4**, 13.

Yarkoni T, Poldrack RA, Nichols TE, Van Essen DC, Wager TD (2011). Large-scale automated synthesis of human functional neuroimaging data. *Nature Methods* **8**, 665–670.

Reproduced with permission of the copyright owner. Further reproduction prohibited without permission.